Supporting Information For DOI: 10.1021/cs.jpca.6b11916: Reactivity of Ketyl and Acetyl Radicals from Direct Solar Actinic Photolysis of Aqueous Pyruvic Acid Publication Date: March 31, 2017

*Alexis J. Eugene and Marcelo I. Guzman**

Department of Chemistry, University of Kentucky, Lexington, Kentucky 40506, Unites States

*Corresponding author's email: marcelo.guzman@uky.edu

The Journal of Physical Chemistry A

Content **Page**

Additional Experimental Section

Fourier transformed infrared (FTIR) Spectroscopy. Gas phase products were analyzed by performing the photolysis in a sealed 200 mL quartz reactor. Aliquots of the headspace above the reaction mixture were withdrawn through a septum using a syringe with a stainless steel needle and injected into a 2.4 m path length infrared gas cell with ZnSe windows (PIKE) and a capacity of 100 cm^3. The cell was mounted in an iZ10 FTIR module connected to an infrared microscope (Thermo Scientific Nicolet iN10). Absorption spectra (and the background) were recorded at 1 cm^{-1} resolution after allowing the cell to equilibrate for 30 min and purging the optics continuously with N_2(g). In addition, photoproducts were spiked with acetoin vapor for qualitative analysis.

UHPLC Analysis of Non-derivatized Samples. Samples were analyzed with the same Accela 1250 LC-MS described in the main experimental section after diluting them 100 times in ultra-pure water. Separation used solvents A (methanol) and B (water) both with 0.1 mM formic acid. Initially a 5% solvent A was kept for 2 min, followed by a 3 min gradient reaching a 50% composition. The samples were spiked with 100 μM salicylic acid (Fluka, 99.6%) as an internal standard. Figure S2 shows good separation of 2,3-dimethyltartaric acid (*m/z* 177.04) and the oxo-C_8 product (*m/z* 219.05) confirming the observation made in Figure 1 of the main paper by IC-MS.

Tandem Mass Spectrometry (MS/MS). Figure S4 shows the fragmentation patterns for pyruvic acid (*m/z* 87), the oxo-C_7 product (*m/z* 175), DMTA (*m/z* 177) and the oxo-C_8 product (*m/z* 219). Figure S4A shows that pyruvic acid fragments into acetic acid (*m/z* 59) by decarbonylation. Figure S4B shows that the oxo-C_7 product easily produces a pyruvic acid like fragment with *m/z* 87 corresponding to $C_3H_3O_3^-$, which is easily obtainable by breaking one of the ether bonds in

the proposed structure shown in Scheme 1 of the main paper. This fragmentation pattern is consistent with what was observed in the past,[1] where it was speculated that the lack of a second ESI(-) detectable fragment indicated there should only be one carboxyl group in the structure of the oxo-C_7 product. The IC-MS analysis presented in Figures 1 and 2 of the main text confirms this conjecture, and demonstrates that the dicarboxylic acid impurity parapyruvic acid (also with *m/z* 175) does not contribute to the MS/MS spectrum of the products. Figure S4C shows the MS/MS of DMTA (*m/z* 177) has fragments at *m/z* 131, 115, and 87, consistent with previous work.[1] In addition, this peak at *m/z* 177 loses a water giving *m/z* 159 and the fragment at *m/z* 115 can decarboxylate to form an ion at *m/z* 71. This secondary decarboxylation provides additional support indicating that the product with *m/z* 177 has two carboxyl groups as in the structure of DMTA. In Figure S4D, the oxo-C_8 product shows multiple ions arising from a labile species. The fragment at *m/z* 201 results from water loss from *m/z* 219. The fragments at *m/z* 175 (matching the oxo-C_7 product) and 157 result from decarboxylation of *m/z* 219 and 201, respectively. Confirmation of the presence of a remaining carboxyl group in *m/z* 175 is shown by its decarboxylation into *m/z* 131. The peak at *m/z* 201 easily breaks into *m/z* 117 by loss of $C_4H_4O_2$ (neutral mass 84 amu) or vice versa generating a weak peak at *m/z* 83 from the loss at 118 amu. The *m/z* 113 fragment can be produced by consecutive loss of a pyruvic acid monomer (88 amu) and water (18 amu) directly from the oxo-C_8 product. This pyruvic acid loss can also be observed at *m/z* 87. Finally, the oxo-C_8 product can fragment into the two halves *m/z* 147 and neutral 72 amu or *m/z* 71 and neutral 148 amu.

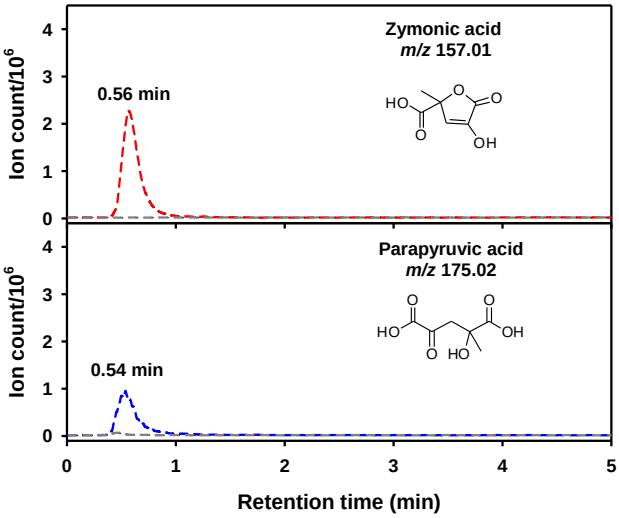

Figure S1. UHPLC-MS extracted ion chromatograms (EIC) for impurities in pyruvic acid reagent. Top panel: EIC at *m/z* 157.01 for zymonic acid (red dashed line) before and (gray dashed line) after vacuum distillation. Bottom panel: EIC at *m/z* 175.02 for parapyruvic acid (blue dashed line) before and (gray dashed line) after vacuum distillation.

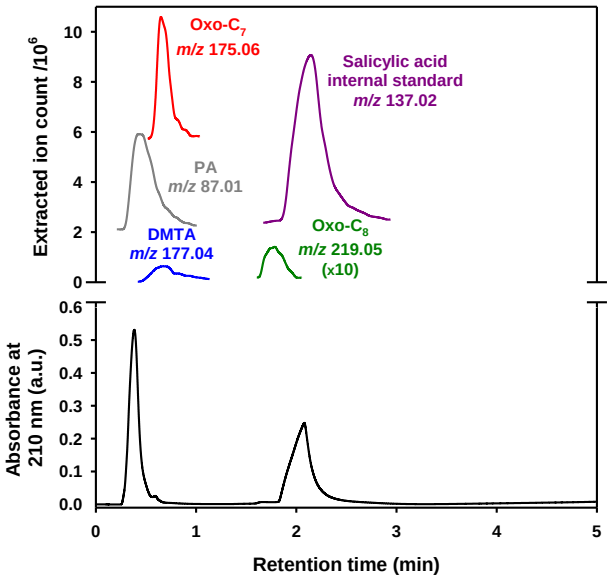

Figure S2. UHPLC (black line) UV chromatogram and ESI(-)/MS EIC for 100.9 mM pyruvic acid photolyzed to a 19.3% conversion. EICs at (gray line) *m/z* 87.01 for pyruvic acid; (red line) *m/z* 175.06 for oxo-C_7 product eluting at 0.65 min, (blue line) *m/z* 177.04 for 2,3-dimethyltartaric acid (DMTA), (green line) *m/z* 219.05 for oxo-C_8 product, and (purple) *m/z* 137.02 for salicylic acid internal standard.

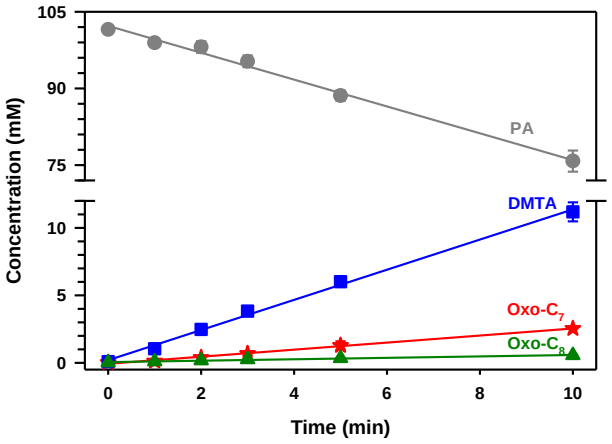

Figure S3. Time series of (gray circle) pyruvic acid loss, (red star) oxo-C_7 product, (blue square) DMTA, and (green triangle) oxo-C_8 product for the experiment in D_2O at pD = 1.0 and 298 K. Initial slopes were used for the calculation of KIE reported in Table 1 of the main text.

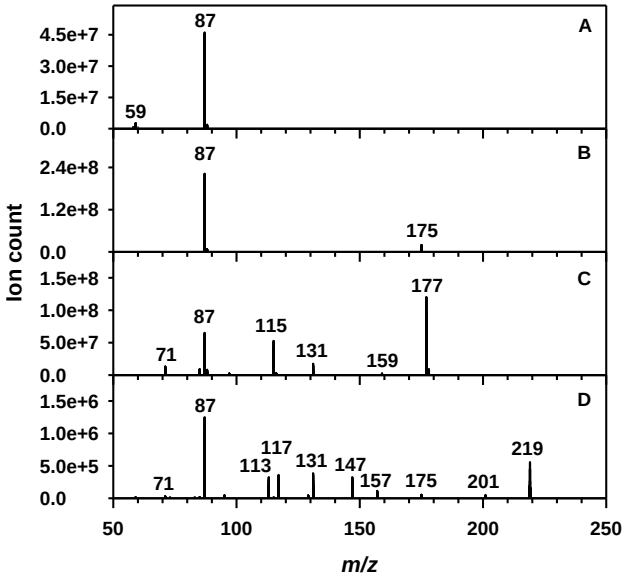

Figure S4. High resolution MS/MS fragmentation patterns for (A) pyruvic acid (*m/z* 87); (B) oxo-C_7 (*m/z* 175); and (C) DMTA (*m/z* 177) in a solution of 100 mM pyruvic acid after photolysis to 20 % conversion.

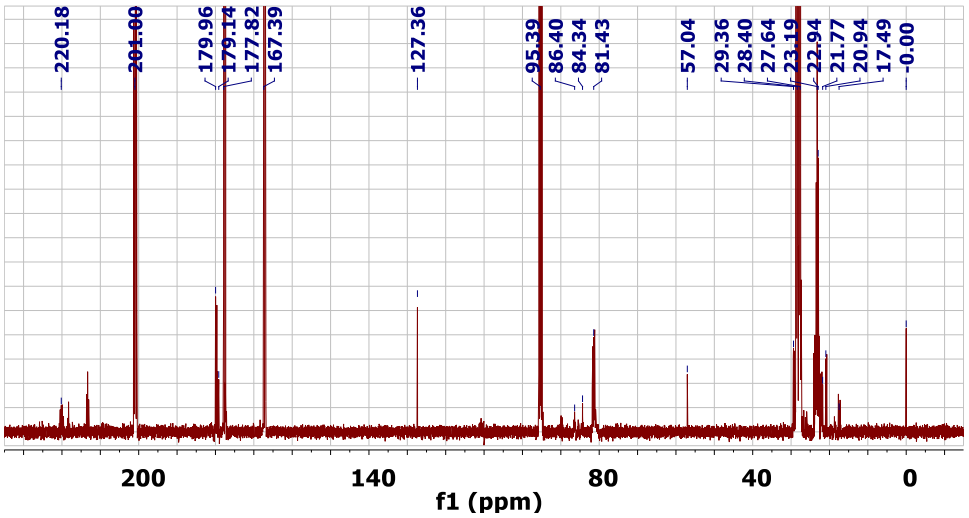

Figure S5. 150 MHz ^{13}C NMR spectrum of 97.9 mM ^{13}C labeled PA at pD = 1.0 for a 9 min photolysis corresponding to a 50.2% conversion.

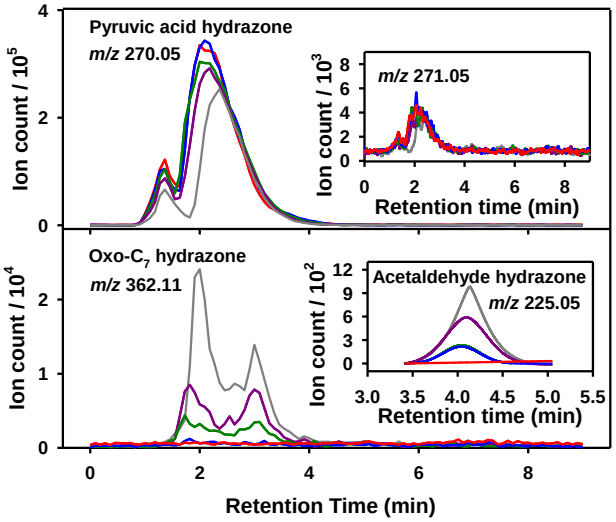

Figure S6. UHPLC-MS chromatograms from hydrazones of (top panel) ^{13}C labeled PA (*m/z* 270.05) and (bottom panel) oxo-C_7 product (*m/z* 362.11) from an experiment with [^{13}C PA] = 115.2 mM photolyzed during (red) 0, (blue) 1, (green) 3, (purple) 5, and (gray) 10 min. Top panel inset: EIC for *m/z* 271.05. Bottom panel inset: Trace production of ^{13}C acetaldehyde (*m/z* 225.05) after smoothing with a Gaussian function.

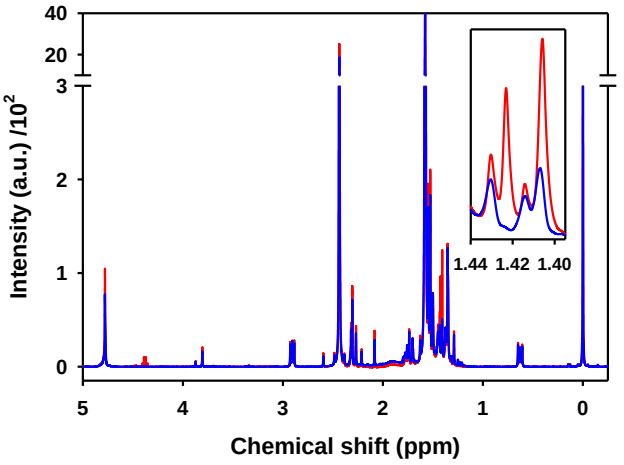

Figure S7. ^{1}H NMR spectrum of 99.9 mM PA photolyzed to 20.0 % conversion (blue) before and (red) after spike addition of lactic acid to a final concentration of 2.24 mM. The inset shows an expansion of the –CH_3 region for the doublet where lactic acid does not overlap well with the signal of the photoproducts.

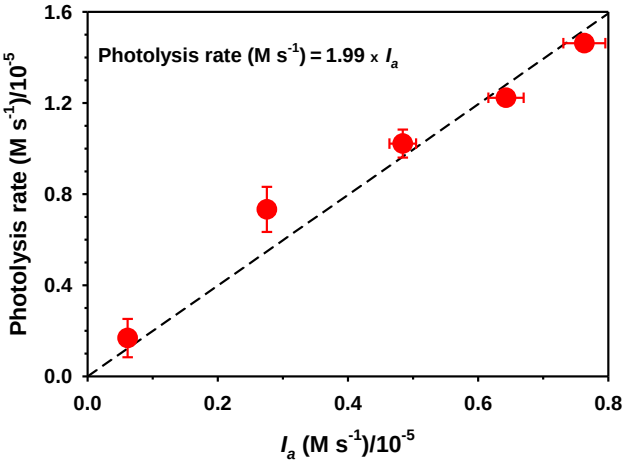

Figure S8. Dependence of the photolytic rate of pyruvic acid, $k_{h\nu} \times [PA]_0$, on the photon absorption rate, I_a, during direct photolysis of aqueous solutions ($\lambda \geq 305$ nm) at pH = 1.0 and 298 K. Incident photon rate $I_0 = 1.14 \times 10^{-5}$ M s^{-1}.

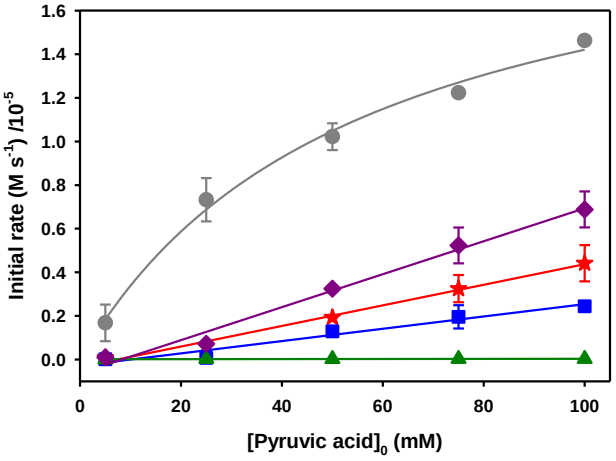

Figure S9. Initial rates of (gray circle) pyruvic acid loss and formation of (red star) the oxo-C_7 product, (blue square) 2,3-dimethyltartaric acid, (green triangle) the oxo-C_8 product, and (purple diamond) the sum for the three products at variable initial pyruvic acid concentration. Experimental conditions are the same reported in Figure S7.

Table S1. Infrared Assignment of Gas Phase Products for Photolyzed ($\lambda \geq 305$ nm) 50 mM Pyruvic Acid in Water, Predicted Oxo-C_7 Product, and Acetoin.[2]

Wavenumber (cm^{-1})			Strength	Assignment
Photolyzed	Oxo-C_7 Product	Acetoin		
1033	1055-870	-	s	C-O-C symmetric stretch
1056	1125-1000	1124	s	C-O stretch, secondary alcohol
1085	1300-1100, 1120	-	s	C-O-C, asymmetric stretch
1316	1320-1210	-	m	C-O stretch, carboxylic acid
1265	1300-1100	1266	m	carbonyl bend
Indist.	1375	1372	s	methyl bend
Indist.	1715	1736	s	C=O stretch, ketone
Indist.	1800-1740	-	s	C=O stretch, carboxylic acid
Indist.	2872	2872	s	methyl C-H symmetric stretch
2967	2962	2987	s	methyl C-H asymmetric stretch
-	3550-3500	-	m	carboxylic acid OH stretch
-	3650-3590	3530	m	O-H stretch

Table S2. Assignment of the 150 MHz ^{13}C NMR spectrum of 97.88 mM fully labeled ^{13}C PA at pD = 1.0 photolyzed for 9 min for a 50.2% conversion.

Chemical shift (ppm)	Assignment[a] (molecule, functionality)
220.18	oxo-C_7, $CH_3\underline{C}(O)CH(CH_3)O$-
201.00	pyruvic acid, $CH_3\underline{C}(O)COOH$
179.96	oxo-C_7, -$C(OH)(CH_3)\underline{C}OOH$
179.14	2,3-dimethyltartaric acid, -$C(OH)(CH_3)\underline{C}OOH$
177.82	gem-diol of pyruvic acid, $CH_3C(OH)_2\underline{C}OOH$
167.39	pyruvic acid, $CH_3C(O)\underline{C}OOH$
127.36	carbon dioxide
95.39	gem-diol of pyruvic acid, $CH_3\underline{C}(OH)_2COOH$
86.40	oxo-C_7, $CH_3C(O)\underline{C}H(CH_3)O$-
84.34	2,3-dimethyltartaric acid, -$\underline{C}(OH)(CH_3)COOH$
81.43	oxo-C_7, -$\underline{C}(OH)(CH_3)COOH$
57.04	DSS, $(CH_3)_3$-Si-CH_2-CH_2-$\underline{C}H_2$-SO_3^-
29.36	oxo-C_7, $\underline{C}H_3C(O)CH(CH_3)O$-
28.40	pyruvic acid, $\underline{C}H_3C(O)COOH$
27.64	gem-diol of pyruvic acid, $\underline{C}H_3C(OH)_2COOH$
23.19	oxo-C_7, $CH_3C(O)CH(\underline{C}H_3)O$-
22.94	oxo-C_7, -$C(OH)(\underline{C}H_3)COOH$
21.77	2,3-dimethyltartaric acid, -$C(OH)(\underline{C}H_3)COOH$
20.94	DSS, $(CH_3)_3$-Si-CH_2-$\underline{C}H_2$-CH_2-SO_3^-
17.49	DSS, $(CH_3)_3$-Si-$\underline{C}H_2$-CH_2-CH_2-SO_3^-
0.000	DSS, $(\underline{C}H_3)_3$-Si-CH_2-CH_2-CH_2-SO_3^-

Table S3. Assignment of the 600 MHz ^{1}H NMR spectrum of 322 mM photolyzed pyruvic acid for a 20.3 % Conversion.

Chemical shift (ppm)	Multiplicity	Assignment[a] (molecule, functionality, diastereomer[b])
4.420	q	oxo-C_7, O-C<u>H</u>-C(O)CH_3, *A* and *B*
2.463	s	pyruvic acid, C<u>H</u>$_3$C=O
2.910	t	DSS, -C<u>H</u>$_2$-SO_3^-
2.322	s	oxo-C_7, O-CH-C(O)C<u>H</u>$_3$, *A*
2.309	s	oxo-C_7, O-CH-C(O)C<u>H</u>$_3$, *B*
2.271	s	C_8, C<u>H</u>$_3$C(O)C-, *A*
2.217	s	C_8, C<u>H</u>$_3$C(O)C-, *B*
2.086	s	acetic acid, C<u>H</u>$_3$COOH
1.686	m	DSS, $(CH_3)_3$-Si-CH_2-C<u>H</u>$_2$-
1.581	s	pyruvic acid gem-diol, C<u>H</u>$_3$C(OH)$_2$
1.551	s	oxo-C_7, O-CH(C<u>H</u>$_3$)-C=O, *A*
1.533	s	2,3-dimethyltartaric acid, HO-C(C<u>H</u>$_3$)-C(C<u>H</u>$_3$)-OH, *A*
1.527	s	oxo-C_7, O-CH(C<u>H</u>$_3$)-C=O, *B*
1.499	s	2,3-dimethyltartaric acid, HO-C(C<u>H</u>$_3$)-C(C<u>H</u>$_3$)-OH, *B*
1.472	s	C_8, HOOC-C(OH)-C<u>H</u>$_3$, *A*
1.451	s, broad	C_8, HOOC-C(OH)-C<u>H</u>$_3$, B and CH_3-C(O)-C-C<u>H</u>$_3$, *A*
1.435	s	C_8, CH_3-C(O)-C-C<u>H</u>$_3$, *B*
1.354	s	oxo-C7, HOOC-C(OH)-C<u>H</u>$_3$, *A* and *B*
0.624	t	DSS, $(CH_3)_3$-Si-C<u>H</u>$_2$-CH_2-
0.000	s	DSS, (C<u>H</u>$_3$)$_3$-Si-

[a]Structures are given in Scheme 1 of the main paper. [b]Two diastereomers (labeled *A* and *B*) exist for each product.

References

(1) Guzman, M. I.; Colussi, A. J.; Hoffmann, M. R. Photoinduced oligomerization of aqueous pyruvic acid. *J. Phys. Chem. A* **2006**, *110*, 3619-3626.

(2) Eugene, A. J.; Xia, S.-S.; Guzman, M. I. Negative production of acetoin in the photochemistry of aqueous pyruvic acid. *Proc. Nat. Acad. Sci. USA* **2013**, *110*, E4274-E4275.